

# Stability of Suspension Bridge I: Aerodynamic and Structural Damping

N.U. AHMED \* and H. HARBI

*Department of Electrical Engineering and Department of Mathematics,  
University of Ottawa, 161 Louis Pasteur st., P.O. Box 450,  
Stn. A, Ottawa, Ontario K1N 6N5, Canada*

*(Received 28 July 1997; In final form 14 November 1997)*

In this paper we consider a few dynamic models of suspension bridge described by partial differential equations with linear and nonlinear couplings. We study analytically the stability properties of these models and the relative effectiveness of aerodynamic and structural damping. Increasing aerodynamic or structural damping indefinitely does not necessarily increase the decay rate indefinitely. In view of possible disastrous effects of high wind, structural damping is preferable to aerodynamic (viscous) damping. These results are illustrated by numerical simulation.

**Keywords:** Suspension bridge; Dynamic models; Stability; Asymptotic stability;  
Numerical results

**AMS Subject Classification:** 34K20; 35Q72; 93D05; 93D20

## 1. INTRODUCTION

Since the collapse of the Tacoma Narrows bridge in the State of Washington on November 7, 1940, extensive studies of the dynamics, stability, oscillation, and occurrence of traveling waves were carried out by many workers in the field [1–13,17,18]. In several papers [1,8,9,10–13], the authors studied the problems of nonlinear oscillations, stability and occurrence of traveling waves. In [1] the authors presented a true PDE model for the suspension bridge that takes account of the fact that

---

\* Corresponding author. Fax: 613-562-5175. E-mail: ahmed@elg.uottawa.ca.

the coupling provided by the stays connecting the suspension cable to the deck of the road bed is fundamentally nonlinear. Stability studies based on PDE models for space structures closely related to the characteristics of suspension bridges were studied in [14–16]. Recently in [17,18] the present authors developed rigorous analysis of suspension bridge based on the PDE models and also studied their stability. Here we study mainly the asymptotic stability, in particular exponential stability, of the structure with reference to aerodynamic and structural damping. This is practically important since a suspension bridge taking long time to settle down to its rest state is not desirable.

## 2. SOME RELEVANT FUNCTION SPACES

Let  $\Sigma \subset R^n$  be an open bounded set with smooth boundary  $\partial\Sigma$  and let  $L_2(\Sigma)$  denote the space of equivalence classes of Lebesgue measurable and square integrable functions with the standard norm topology. Let  $H^m(\Sigma) \equiv H^m$ ,  $m \in N$ , denote the standard Sobolev space with the usual norm topology

$$\|\psi\|_{H^m} \equiv \sum_{|\alpha| \leq m} \|D^\alpha \psi\|_{L_2(\Sigma)}, \quad \alpha = (\alpha_1, \alpha_2, \dots, \alpha_n), \quad \alpha_i \geq 0, \quad |\alpha| \equiv \sum \alpha_i$$

and  $H_0^m(\Sigma) \equiv H_0^m \subset H^m$  denote the completion in the topology of  $H^m$  of  $C^\infty$  functions on  $\Sigma$  with compact support. From classical results on Sobolev spaces it is well known that the elements of  $H_0^m$  are those of  $H^m$  which, along with their conormal derivatives up to order  $m-1$ , vanish on the boundary  $\partial\Sigma$ .

## 3. DYNAMIC MODELS OF SUSPENSION BRIDGE

### *Suspension Bridge Model*

A simplified model of a suspension bridge is given by a coupled system of partial differential equations of the form

$$\begin{aligned} m_b z_{tt} + \alpha D^4 z - F_0(y - z) &= m_b g + f_1, \quad x \in (0, \ell) \equiv \Sigma, \quad t \geq 0; \\ m_c y_{tt} - \beta D^2 y + F_0(y - z) &= m_c g + f_2, \quad x \in (0, \ell), \quad t \geq 0, \end{aligned} \quad (3.1)$$

where the first equation describes the vibration of the road bed in the vertical plain and the second equation describes that of the main cable from which the road bed is suspended by tie cables (stays).  $D^k$  denotes the spatial derivative of order  $k$ . Here  $m_b, m_c$  are the masses per unit length of the road bed and the cable respectively;  $\alpha, \beta$  are the flexural rigidity of the structure and coefficient of elasticity or stiffness of the cable respectively. The function  $F_0$  represents the restraining force experienced both by the road bed and the suspension cable as transmitted through the tie lines (stays) thereby producing the coupling between the two. The functions  $f_1$  and  $f_2$  represent external as well as nonconservative forces generally time dependent. Let  $z_s, y_s$  represent the static displacements (equilibrium positions) which are the solutions of the system of equations:

$$\begin{aligned} \alpha D^4 z - F_0(y - z) &= m_b g, & x \in (0, \ell); \\ -\beta D^2 y + F_0(y - z) &= m_c g, & x \in (0, \ell), \end{aligned} \quad (3.2)$$

subject to any one of the following set of boundary conditions. If the decks are clamped at both ends the boundary conditions are given by

$$\begin{aligned} z(t, 0) &= z(t, \ell) = 0, & Dz(t, 0) = Dz(t, \ell) = 0, \\ y(t, 0) &= y(t, \ell) = 0. \end{aligned} \quad (3.3a)$$

In case they are hinged at both ends the boundary conditions are given by

$$\begin{aligned} z(t, 0) &= z(t, \ell) = 0, & D^2 z(t, 0) = D^2 z(t, \ell) = 0, \\ y(t, 0) &= y(t, \ell) = 0. \end{aligned} \quad (3.3b)$$

Other combinations, such as hinged on one side and clamped on the other, are also used. The initial conditions are

$$\begin{aligned} z(0, x) &= z_0(x), & z_t(0, x) = z_1(x), \\ y(0, x) &= y_0(x), & y_t(0, x) = y_1(x). \end{aligned} \quad (3.4)$$

Subtracting Eq. (3.2) from (3.1) we obtain the following system of equations:

$$\begin{aligned} m_b \tilde{z}_{tt} + \alpha D^4 \tilde{z} - F(\tilde{y} - \tilde{z}) &= f_1, & x \in \Sigma \equiv (0, \ell), t \geq 0; \\ m_c \tilde{y}_{tt} - \beta D^2 \tilde{y} + F(\tilde{y} - \tilde{z}) &= f_2, & x \in (0, \ell), t \geq 0, \end{aligned} \quad (3.5)$$

where  $\tilde{z} \equiv z - z_s$ ,  $\tilde{y} \equiv y - y_s$  and the function  $F$  is given by

$$F(\zeta) \equiv F_0(\zeta + z_s - y_s) - F_0(z_s - y_s).$$

Note that  $F(0) = 0$ . Throughout the rest of the paper we assume that the displacements, again denoted by  $z, y$  instead of  $\tilde{z}, \tilde{y}$ , are measured relative to the static positions. We use (3.5) as the general model.

## Conservative Systems

### (3A) Linear Model

In case the tie cables never loose tension, the restraining force  $F$  is given by

$$F(\xi) = k\xi,$$

where  $k$  is the stiffness coefficient of the vertical cables and  $\xi$  represents their elongation from the equilibrium. In this case, in the absence of external force, the dynamics of the suspension bridge around the equilibrium position is described by a system of coupled linear partial differential equations as given below:

$$\begin{aligned} m_b z_{tt} + \alpha D^4 z - k(y - z) &= 0, \quad x \in (0, \ell), \quad t \geq 0; \\ m_c y_{tt} - \beta D^2 z - k(y - z) &= 0, \quad x \in (0, \ell), \quad t \geq 0. \end{aligned} \quad (3.6)$$

The same linear model is obtained if the road bed is assumed to be supported with ties (stays) connected to two symmetrically placed main (suspension) cables one above and one below the road bed. The initial conditions are given by

$$\begin{aligned} z(0, x) &= z_1(x), \quad z_t(0, x) = z_2(x), \quad x \in (0, \ell), \\ y(0, x) &= y_1(x), \quad y_t(0, x) = y_2(x), \quad x \in (0, \ell), \end{aligned} \quad (3.7)$$

where  $z_1, z_2, y_1, y_2$  are suitable real valued functions defined on  $\Sigma = (0, \ell)$ . Using any one of the boundary conditions (3.3) or (3.4), one can establish the existence and uniqueness of solutions of the system (3.6)–(3.7) [17]. Given that  $z_1 \in H_0^2$ ,  $z_2 \in L_2(\Sigma)$ ,  $y_1 \in H_0^1$  and  $y_2 \in L_2(\Sigma)$  the system (3.4)–(3.7) has a unique solution  $\{z, y\} \in L_\infty(I, H_0^2 \times H_0^1)$  and  $\{z_t, y_t\} \in L_\infty(I, L_2(\Sigma) \times L_2(\Sigma))$ .

The total system energy is given by

$$E(t) \equiv (1/2) \int_0^\ell \left\{ m_b |z_t|^2 + m_c |y_t|^2 + \alpha |D^2 z|^2 + \beta |Dy|^2 + k |(y - z)|^2 \right\} dx, \quad (3.8)$$

where the first two terms represent the kinetic energies of the deck and the main suspension cables respectively and the next two terms represent their elastic potential energies and the fifth term represents the elastic energy due to tension in the vertical cables. Differentiating  $E$  with respect to time and using the boundary conditions (3.3) or (3.4) we obtain

$$\begin{aligned} (d/dt)E = \int_0^\ell & \left\{ (m_b z_{tt} + \alpha D^4 z - k(y - z))z_t \right. \\ & \left. + (m_c y_{tt} + \beta D^2 y + k(y - z))y_t \right\} dx. \end{aligned}$$

Since the couple  $\{z, y\}$  is the solution of the system (3.6)–(3.7), it follows from the above expression that  $(d/dt)E = 0$  and hence

$$E(t) = E(0), \quad \text{for all } t \geq 0. \quad (3.9)$$

This shows that the homogeneous system (3.6)–(3.7) with either one of the boundary conditions (3.3) or (3.4) is conservative and hence stable in the Lyapunov sense. However the system is not asymptotically stable with respect to the rest state though this is what is desirable for engineering structures. In fact in the absence of other external forces, other than the initial disturbance (which may have been caused by sudden wind gust or seismic activity), the system will continue to oscillate unabated.

### **(3B) Nonlinear Model**

If the tie cables (stays) experience loss of tension the system is no more linear and one must consider Eq. (3.5) with  $F$  nonlinear. In particular,  $F$  may be taken as  $F(\xi) = k\Psi(\xi)$  where

$$\Psi(\xi) = \begin{cases} \xi, & \text{if } \xi > 0, \\ 0, & \text{otherwise.} \end{cases} \quad (3.10)$$

This replaces the linear model (3.6) by the following nonlinear system:

$$\begin{aligned} m_b z_{tt} + \alpha D^4 z - k\Psi(y - z) &= 0, \quad x \in \Sigma \equiv (0, \ell), \quad t \geq 0; \\ m_c y_{tt} - \beta D^2 y + k\Psi(y - z) &= 0, \quad x \in (0, \ell), \quad t \geq 0. \end{aligned} \quad (3.11)$$

This is subject to the same set of boundary and initial conditions (3.3)–(3.4) and (3.7) respectively. Note that the model (3.11) takes into account the fact that there are no restraining forces whenever the stays (tie cables) are loose. In other words when the stays are loose the road bed is decoupled from the main cables. This may also arise in case of symmetrically supported road bed, if one of the set of tie cables above or below the road bed suddenly breaks loose. In any event the total system energy is given by

$$\begin{aligned} E(t) \equiv (1/2) \int_0^\ell & \left\{ m_b |z_t|^2 + m_c |y_t|^2 + \alpha |D^2 z|^2 + \beta |Dy|^2 \right. \\ & \left. + k(\Psi(y - z))^2 \right\} dx. \end{aligned} \quad (3.12)$$

Differentiating this with respect to time and using the boundary conditions (3.3) while integrating by parts, one can verify that

$$\begin{aligned} (d/dt)E(t) = \int_0^\ell & \left\{ (m_b z_{tt} + \alpha D^4 z - k\Psi(y - z))z_t \right. \\ & \left. + (m_c y_{tt} + \beta D^2 y + k\Psi(y - z))y_t \right\} dx. \end{aligned}$$

Thus it follows from Eq. (3.11) and the above expression that

$$\dot{E}(t) = 0 \quad (3.13)$$

and hence the nonlinear system is also conservative. Again this implies stability in the Lyapunov sense only and since there is no dissipation of energy, the system will continue to vibrate perpetually once a jolt of energy is delivered to the structure.

### **(3C) General Nonlinear Model**

In general the function  $F$  of model (3.5) can be taken as any function with its graph lying in the first and third quadrants of the plane  $R^2$ . However from physical point of view it makes sense only if  $F$  is a

nondecreasing function of its argument. In other words this simply means that a positive amount of energy is required for stretching any elastic cable till it reaches its plastic state and breaks down. In any case let us consider the corresponding homogeneous system:

$$\begin{aligned} m_b z_{tt} + \alpha D^4 z - F(y - z) &= 0, \quad x \in \Sigma \equiv (0, \ell), \quad t \geq 0; \\ m_c y_{tt} - \beta D^2 y + F(y - z) &= 0, \quad x \in (0, \ell), \quad t \geq 0. \end{aligned} \quad (3.14)$$

This is subject to the same set of boundary and initial conditions as in (3.3)–(3.4) and (3.7) respectively. Define

$$G(\zeta) \equiv \int_0^\zeta F(\xi) d\xi. \quad (3.15)$$

The total system energy is then given by

$$E(t) \equiv (1/2) \int_0^\ell \left\{ m_b |z_t|^2 + m_c |y_t|^2 + \alpha |D^2 z|^2 + \beta |Dy|^2 + 2G(y - z) \right\} dx. \quad (3.16)$$

Again it is easy to verify that

$$\dot{E}(t) = 0 \quad (3.17)$$

and hence the nonlinear system (3.14) is also conservative and the previous conclusions hold.

We summarize the above results in the form a theorem.

**THEOREM 1** *In the absence of external forces, a suspension bridge, linear or nonlinear, is conservative. The total energy functionals given by (3.8) for the linear system, (3.12) for a simple nonlinearity and (3.16) for the general nonlinear system, are Lyapunov functions for the respective systems and these systems are stable in the Lyapunov sense.*

## Nonconservative Systems

### (3D) Aerodynamic Damping

In all the models given above aerodynamic damping was neglected. Natural atmosphere surrounding the structure provides viscous damping. Considering the general model (3.5) and including the

viscous damping (aerodynamic damping) we have

$$\begin{aligned} m_b z_{tt} + \alpha D^4 z - F(y - z) &= f_1(z_t), \quad x \in \Sigma \equiv (0, \ell), \quad t \geq 0; \\ m_c y_{tt} - \beta D^2 y + F(y - z) &= f_2(y_t), \quad x(0, \ell), \quad t \geq 0, \end{aligned} \quad (3.18)$$

where  $f_1$  and  $f_2$  are suitable functions of displacement rates. This is subject to the same set of boundary and initial conditions as in (3.3) and (3.7) respectively. Using the energy function (3.16) and carrying out the differentiation and integrating by parts while using the boundary condition (3.3) one can verify that

$$(\mathrm{d}/\mathrm{d}t)E(t) = \int_0^\ell \{f_1(z_t)z_t + f_2(y_t)y_t\} \, dx. \quad (3.19)$$

It follows from this expression that if  $f_i(\xi)\xi \leq 0$  then  $\dot{E} \leq 0$ . It can be shown [17] that the system is asymptotically stable with respect to the rest state, given that  $f_i(0) = 0$ ,  $f_i(\zeta)\zeta < 0$ , for  $\zeta \neq 0$ , and  $F(\xi)\xi \geq 0$ , for  $\xi \in R$ . In other words, if the graphs of the functions  $-f_i$  and  $F$  lie in the open first and third quadrants of the plane then the equilibrium state is asymptotically stable. For detailed proof see [17]. This stability property also holds for linear aerodynamic damping with  $f_1(\xi) = -\gamma_1\xi$ ,  $f_2(\xi) = -\gamma_2\xi$ . In this case Eq. (3.19) reduces to

$$(\mathrm{d}/\mathrm{d}t)E(t) = \int_0^\ell \left\{ \gamma_1|z_t|^2 + \gamma_2|y_t|^2 \right\} \, dx, \quad (3.20)$$

where  $\gamma_1, \gamma_2 > 0$ , are the aerodynamic coefficients of the road bed and the main cables respectively. Of course these constants are dependent on the geometry, particularly the effective surface area resisting free air flow, and not the constituent materials. Thus one cannot indefinitely increase the aerodynamic damping. Further it is also not desirable since wind actions can destabilize the system. The fact that arbitrary increase of aerodynamic damping does not increase the damping rate can be justified as follows. For simplicity we consider the linear version of (3.18):

$$\begin{aligned} m_b z_{tt} + \alpha D^4 z + K(z - y) + \gamma_1 z_t &= 0, \quad x \in \Sigma \equiv (0, \ell), \quad t \geq 0; \\ m_c y_{tt} - \beta D^2 y + K(y - z) + \gamma_2 y_t &= 0, \quad x \in (0, \ell), \quad t \geq 0. \end{aligned} \quad (3.21)$$

Following the same procedure as in [17], we can reformulate this system as an ordinary differential equation on the Hilbert space  $H \equiv L_2(\Sigma) \times L_2(\Sigma)$ :

$$\ddot{\phi} + A\phi + KB\phi + \alpha\dot{\phi} = 0, \quad \phi(0) = \Theta_1, \quad \dot{\phi}(0) = \Theta_2. \quad (3.22)$$

Here

$$\phi(t) \equiv \begin{pmatrix} z(t, \cdot) \\ y(t, \cdot) \end{pmatrix}$$

denotes the instantaneous displacement profiles of the road bed and the main cables along the span of the bridge respectively and  $\Theta_1$  and  $\Theta_2$  denote the initial displacement profile and its rate. The operator  $A$  is given by the realization of the formal differential operator

$$A(D)\phi \equiv \begin{pmatrix} a^2 D^4 \phi_1 \\ -b^2 D^2 \phi_2 \end{pmatrix} \quad (3.23)$$

subject to the boundary conditions (3.3) or (3.4). The operator  $A$  is a positive self-adjoint unbounded operator in  $H$  and  $-A$  generates a  $C_0$  semigroup of contractions. The operator  $B$  is given by

$$B\phi \equiv \begin{pmatrix} 1/m_b & -1/m_b \\ -1/m_c & 1/m_c \end{pmatrix} \begin{pmatrix} \phi_1 \\ \phi_2 \end{pmatrix}.$$

For simplicity of presentation the parameter  $\alpha$  is assumed to be given by

$$\alpha \equiv (\gamma_1/m_b) = (\gamma_2/m_c).$$

Note that the boundary conditions are absorbed in the space  $V \equiv H_0^2 \times H_0^1$ . Thus using this space one can treat the differential operator  $A$  as a bounded operator from  $V$  to its dual  $V^*$ . That is,  $A \in \mathcal{L}(V, V^*)$  and one can easily verify that for  $\delta \equiv \min\{a^2, b^2\}$

$$\langle A\phi, \phi \rangle_{V^*, V} \geq \delta \|\phi\|_V^2, \quad (3.24)$$

or in other words  $A$  is coercive. Since  $V$  is continuously embedded in  $H$  there exists a constant  $c > 0$  such that

$$\|h\|_H \leq c\|h\|_V \quad \text{for all } h \in V. \quad (3.25)$$

We may assume that  $c$  is the smallest such constant. Hence it follows from (3.24) and (3.25) that

$$\langle A\phi, \phi \rangle_{V^*, V} \geq (\delta/c^2)\|\phi\|_H^2,$$

and therefore the smallest eigenvalue of the operator  $A$  given by

$$\nu_1 \equiv \inf \left\{ \langle A\phi, \phi \rangle_{V^*, V}, \|\phi\|_H = 1 \right\} \quad (3.26)$$

has the lower bound  $\nu_1 \geq (\delta/c^2) > 0$ . Now considering the operator  $\tilde{A} \equiv (A + KB)$  it is easy to see that

$$\langle \tilde{A}\phi, \phi \rangle_{V^*, V} \geq (\delta/c^2) - (K/2)(m_b - m_c/m_b m_c). \quad (3.27)$$

Thus if

$$(\delta/c^2) - (K/2)(m_b - m_c/m_b m_c) > 0,$$

the smallest eigenvalue, say  $\lambda_1$ , of the operator  $\tilde{A}$  is positive and

$$\lambda_1 \geq (\delta/c^2) - (K/2)(m_b - m_c/m_b m_c). \quad (3.28)$$

Then it follows from a well known result (see [19, Proposition 1.2, p. 179]) that for

$$d \equiv (1/2) \min\{\alpha/4, \lambda_1/2\alpha\} \quad (3.29)$$

the linear system (3.22) and hence (3.21) is exponentially stable with the decay rate  $d$  or equivalently

$$\|\phi(t)\|_V^2 + \|\dot{\phi}(t)\|_H^2 \leq c_0^2 e^{-dt}, \quad t \geq 0. \quad (3.30)$$

Define the state space as  $E \equiv V \times H$  with the norm topology

$$\|\zeta\|_E \equiv \left( \|\zeta_1\|_V^2 + \|\zeta_2\|_H^2 \right)^{1/2}$$

induced by the natural scalar product. This is a Hilbert space. Using this state space one can rewrite Eq. (3.22) as a first order evolution equation in  $E$

$$\dot{\psi} = \begin{pmatrix} 0 & I \\ -\tilde{A} & -\alpha I \end{pmatrix} \psi, \quad (3.31)$$

where  $\psi \equiv \begin{pmatrix} \phi \\ \dot{\phi} \end{pmatrix}$  denotes the state covering both the displacement and its rate profiles. Hence the expression (3.30) can be presented as

$$\|\psi(t)\|_E \leq c_0 e^{-(d/2)t}, \quad t \geq 0. \quad (3.32)$$

It is evident from Eq. (3.29) that the decay rate  $d$  cannot be indefinitely increased by increasing the aerodynamic damping coefficient  $\alpha$  or equivalently the coefficients  $\{\gamma_1, \gamma_2\}$ . Maximum  $d$  is obtained when the two factors in (3.29) are equal giving the best aerodynamic damping  $\alpha = \sqrt{(2\lambda_1)}$  and the corresponding decay rate  $d_m \equiv \sqrt{(\lambda_1/2)}$ . If one includes only structural damping, assuming aerodynamic damping negligible, Eq. (3.22) changes to

$$\ddot{\phi} + A\phi + KB\phi + \gamma_{12}C\dot{\phi} = 0, \quad \phi(0) = \Theta_1, \quad \dot{\phi}(0) = \Theta_2, \quad (3.22)'$$

where  $\gamma_{12}$  is the coefficient of structural damping and the operator  $C$  is given by

$$C \equiv \begin{pmatrix} -D^2 & 0 \\ 0 & 0 \end{pmatrix}.$$

Again, indefinite increase of structural damping  $\gamma_{12}$  does not increase the decay rate. Here also there is an optimum value. We state these results in the following theorem.

**THEOREM 2** *In the presence of either aerodynamic damping or structural damping, a suspension bridge, linear or nonlinear, is asymptotically stable. The total energy functional is a Lyapunov function for the system. The rate of decay cannot be indefinitely improved by increasing the damping coefficients; there is an optimum value and any deviation from this will cause a decrease in the decay rate.*

The statements of this theorem are illustrated by numerical simulation results shown in Figs. 1, 2, 5, 6, 9 and 10 as explained in Section 4.

### (3E) Structural Plus Aerodynamic Damping

In the presence of both viscous and structural damping  $f_1$  is a function of  $z_t$ ,  $D^2z_t \equiv (\partial/\partial t)(D^2z)$  and possibly also  $D^4z_t$ . Assuming linearity  $f_1$  may be given by

$$f_1(z_t, D^2z_t, D^4z_t) = -\gamma_1 z_t + \gamma_{12} D^2z_t - \gamma_{13} D^4z_t. \quad (3.33)$$

The coefficients  $\gamma_{12}$  and  $\gamma_{13}$  are dependent on the metallurgical properties of the construction materials while  $\gamma_1$  is dependent on the geometry of the road bed, for example, the surface area, shape etc. For the suspension cable structural damping is negligible. Assuming linear viscous damping  $f_2$  is given by

$$f_2(y_t) = -\gamma_2 y_t. \quad (3.34)$$

Clearly from physical consideration damping coefficients are non-negative and hence  $\gamma_1, \gamma_{12}, \gamma_{13}, \gamma_2 \geq 0$ . Substituting these in Eq. (3.18), with  $f_1$  and  $f_2$  now given by (3.33) and (3.34) it follows from (3.19) that

$$\dot{E}(t) = - \int_0^{\ell} \left\{ \gamma_1 \geq |z_t|^2 + \gamma_{12} |Dz_t|^2 + \gamma_{13} |D^2z_t|^2 + \gamma_2 |y_t|^2 \right\} dx \leq 0. \quad (3.35)$$

Thus material properties can provide additional damping. From (3.35) one can justify that the system is asymptotically stable with respect to the origin.

If one includes both structural and aerodynamic damping, assuming the higher order structural damping negligible,  $\gamma_{13} = 0$ , Eq. (3.22) changes to

$$\ddot{\phi} + A\phi + KB\phi + (\alpha I + \gamma_{12}C)\dot{\phi} = 0, \quad \phi(0) = \Theta_1, \quad \dot{\phi}(0) = \Theta_2, \quad (3.22)''$$

where both  $\alpha \neq 0$  and  $\gamma_{12} \neq 0$ . The combined effect is much more effective. We state this result in the form of a theorem.

**THEOREM 3** *In the presence of both aerodynamic and structural damping, a suspension bridge, linear or nonlinear, is asymptotically stable. The total energy functional is a Lyapunov function for the system. The decay rate can be improved by suitable choice of the coefficients  $\{\alpha, \gamma_{12}\}$ .*

#### 4. NUMERICAL RESULTS AND DISCUSSIONS

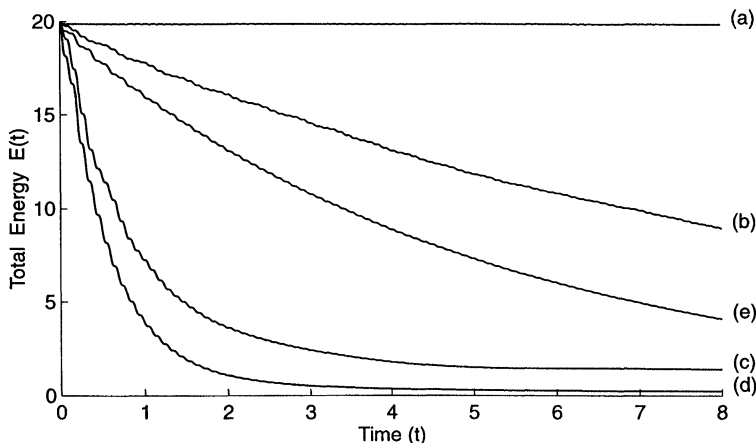
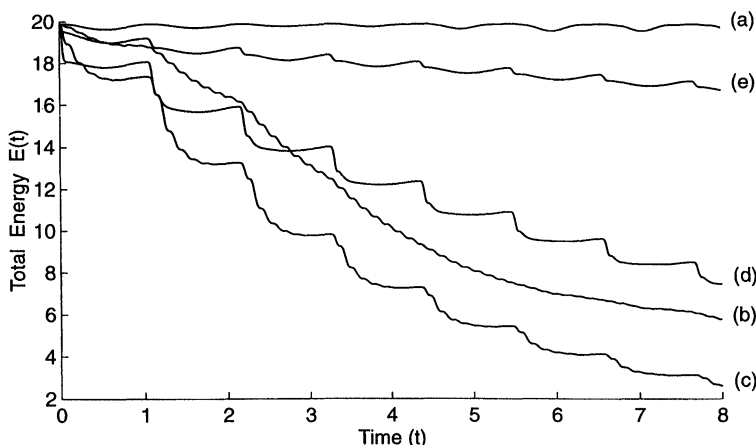
In view of the above results, designers can choose suitable construction materials for the road bed as well as its geometry (perforated or solid) to provide sufficient damping so as to obtain desirable decay rate thereby providing speedy dissipation of energy. This will minimize the possibility of failure due to fatigue caused by oscillation for extended period of time. Here there is a possibility of trade-off between structural damping and aerodynamic damping. It is clearly desirable to trade aerodynamic damping for structural damping in regions that experience frequent storms or turbulent weather. Further as indicated above aerodynamic damping can neither be indefinitely increased nor it is desirable to do so. But structural damping can be increased by choice of so-called "smart" materials for construction of the decks. However indefinite increase of structural damping also does not necessarily increase the decay rate indefinitely as stated in Theorem 2.

We present here some simulation results indicating the effectiveness of the two processes of damping. According to Eqs. (3.9), (3.13) and (3.17) it is evident that in the absence of any damping, aerodynamic or structural, a suspension bridge is conservative irrespective of whether it is linear or nonlinear. This is illustrated by the total energy plots as shown in Figs. 1(a), 5(a), 9(a), 13(a) and 15(a) for linear system and Figs. 2(a), 6(a), 10(a), 14(a) and 16(a) for nonlinear systems. The damping parameters used for each of the cases a, b, c, d, e are shown in the graphs with the first column giving the values of  $\gamma_1$ , the second entry giving the values of  $\gamma_2$  and the third giving the values of  $\gamma_{1,2}$ .

##### **(4A) Decay Rate vs Aerodynamic Damping (Roadbed) $\gamma_1$**

The aerodynamic damping coefficient of the roadbed is denoted by  $\gamma_1$ . The results are shown (see Figs. 1 and 2) for increasing values of  $\gamma_1$

	$\gamma_1$	$\gamma_2$	$\gamma_{12}$
a:	0	0	0
b:	$10^{-5}$	0	0
c:	$10^{-4}$	0	0
d:	$10^{-3}$	0	0
e:	$10^{-2}$	0	0

FIGURE 1 Linear case with viscous damping ( $\gamma_1$ ).FIGURE 2 Nonlinear case with viscous damping ( $\gamma_1$ ).

starting from zero indicated by  $a \rightarrow b \rightarrow c \rightarrow d \rightarrow e$ . For the linear system, as the aerodynamic coefficient  $\gamma_1$  is increased the decay rate improves up to a certain value and reaches a maximum and then declines with further increase of  $\gamma_1$ . This is shown in Fig. 1 for the linear system. The value of  $\gamma_1$  corresponding to the plot (d) is the best and further increase of  $\gamma_1$  produces the graph (e) showing the decline in decay rate. Similar results for the nonlinear system are shown in Fig. 2. Here  $\gamma_1$  corresponding to the graph Fig. 2(c) is the best. Further increase of  $\gamma_1$  produces the plots (d) and (e) showing the increasing decline of the decay rate. The displacements and their rates are plotted in Fig. 3 for the linear system and Fig. 4 for the nonlinear system. These

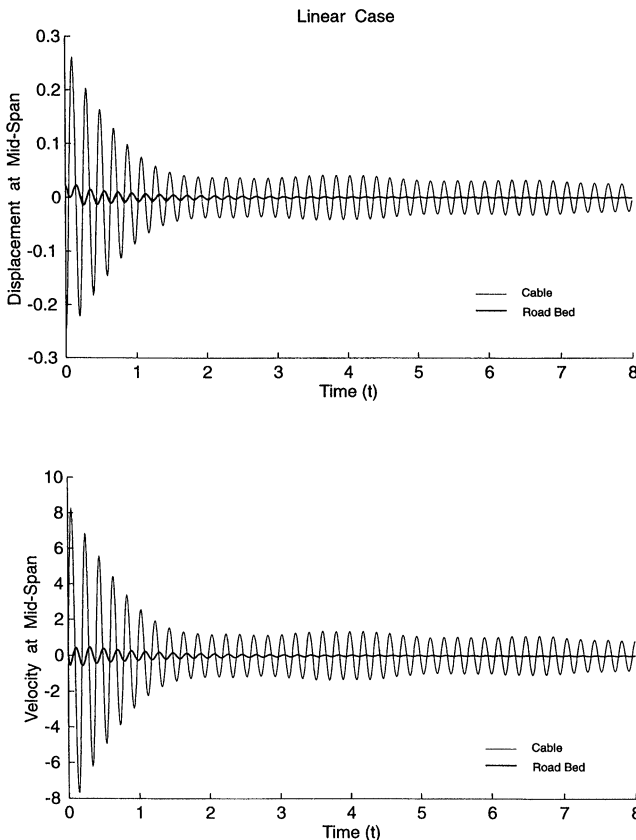


FIGURE 3 Displacement & velocity for  $\gamma_1 = 10^{-3}$ .

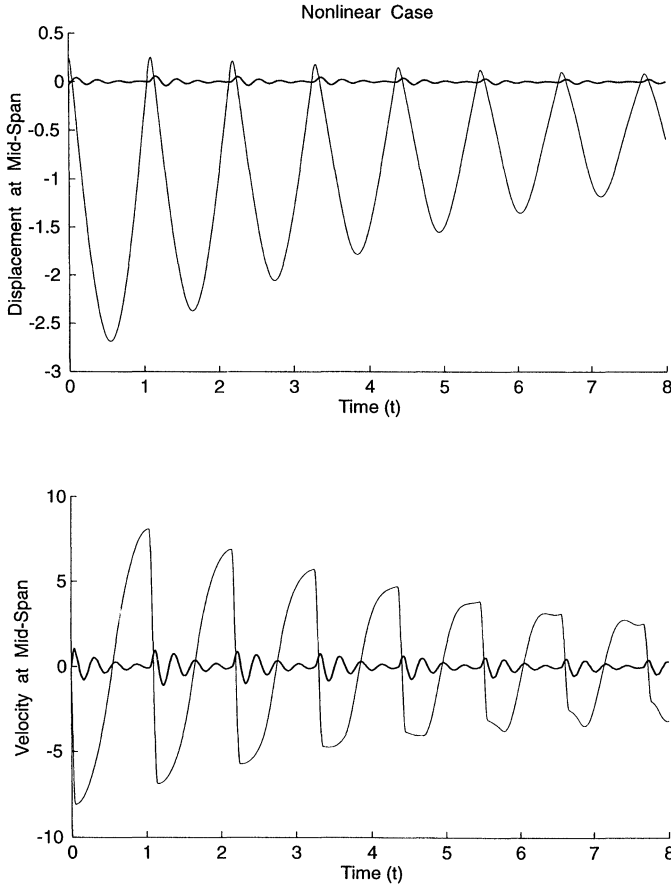


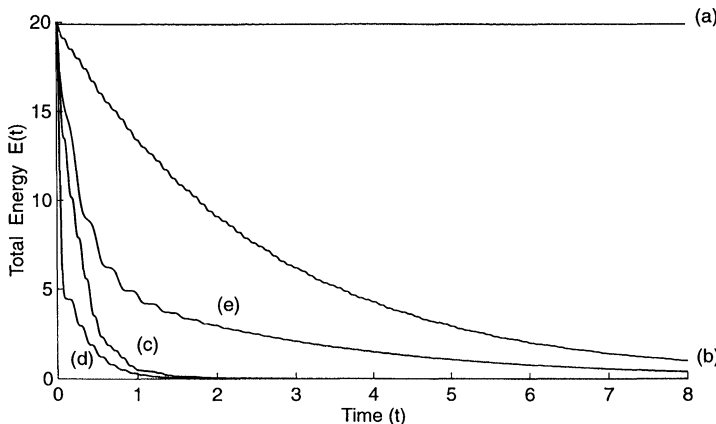
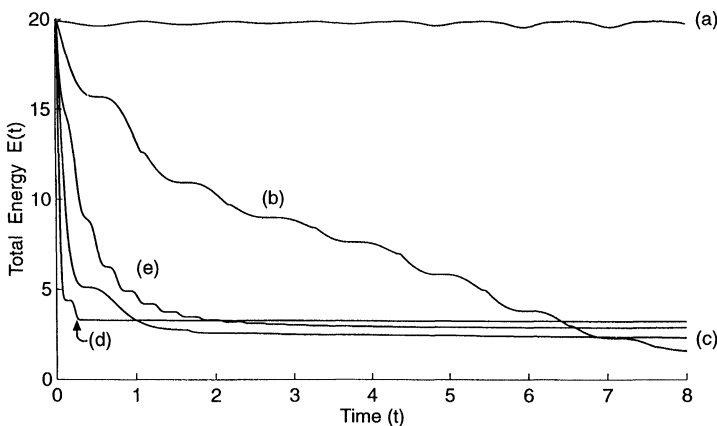
FIGURE 4 Displacement & velocity for  $\gamma_1 = 10^{-4}$ .

results clearly demonstrate that the decay rate cannot be indefinitely improved by simply increasing the aerodynamic damping coefficient. This supports the theory presented in Section 3.

#### (4B) Decay Rate vs Aerodynamic Damping (Main Cables) $\gamma_2$

The aerodynamic damping coefficient of the suspension cables is denoted by  $\gamma_2$ . The corresponding energy decay is shown in Fig. 5 for the linear system and Fig. 6 for the nonlinear system. The results are

	$\gamma_1$	$\gamma_2$	$\gamma_{12}$
a:	0	0	0
b:	0	$10^{-5}$	0
c:	0	$10^{-4}$	0
d:	0	$10^{-3}$	0
e:	0	$10^{-2}$	0

FIGURE 5 Linear case with viscous damping ( $\gamma_2$ ).FIGURE 6 Nonlinear case with viscous damping ( $\gamma_2$ ).

shown for increasing values of  $\gamma_2$  starting from zero indicated by  $a \rightarrow b \rightarrow c \rightarrow d \rightarrow e$ . The graphs Figs. 5(a) and 6(a) represent the cases without damping. Again the Figs. 5(b)–(e) and 6(b)–(e) show the energy decay for increasing values of damping coefficient. Note that the decay rate attains its maximum and then starts declining with further increase of the coefficient. Figs. 7 and 8 show the displacements and their rates for the linear and the nonlinear systems respectively. Again these results clearly demonstrate that the decay rate cannot be

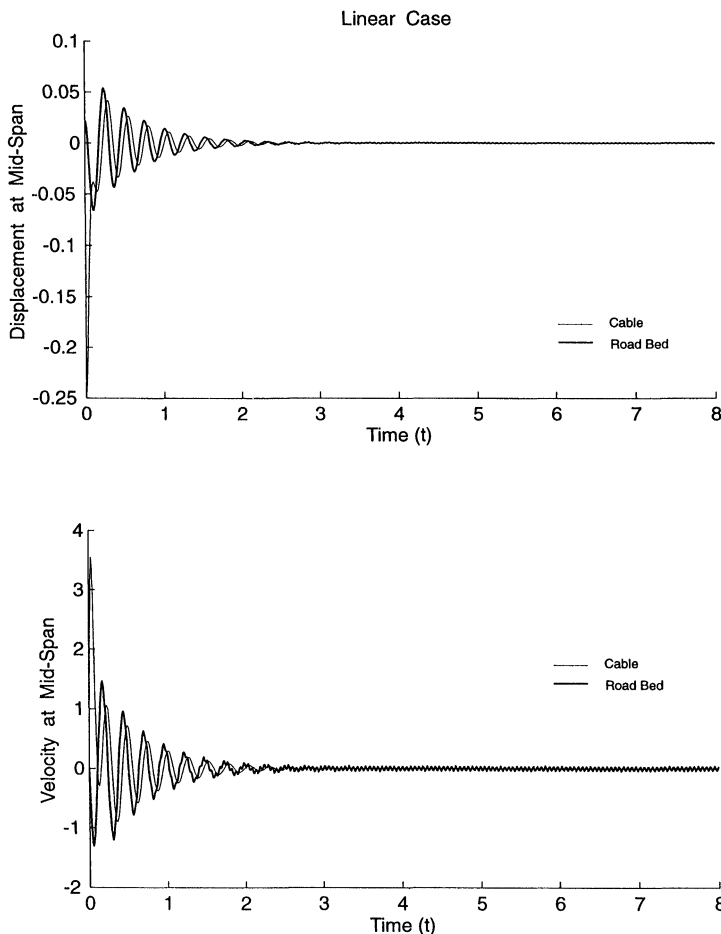
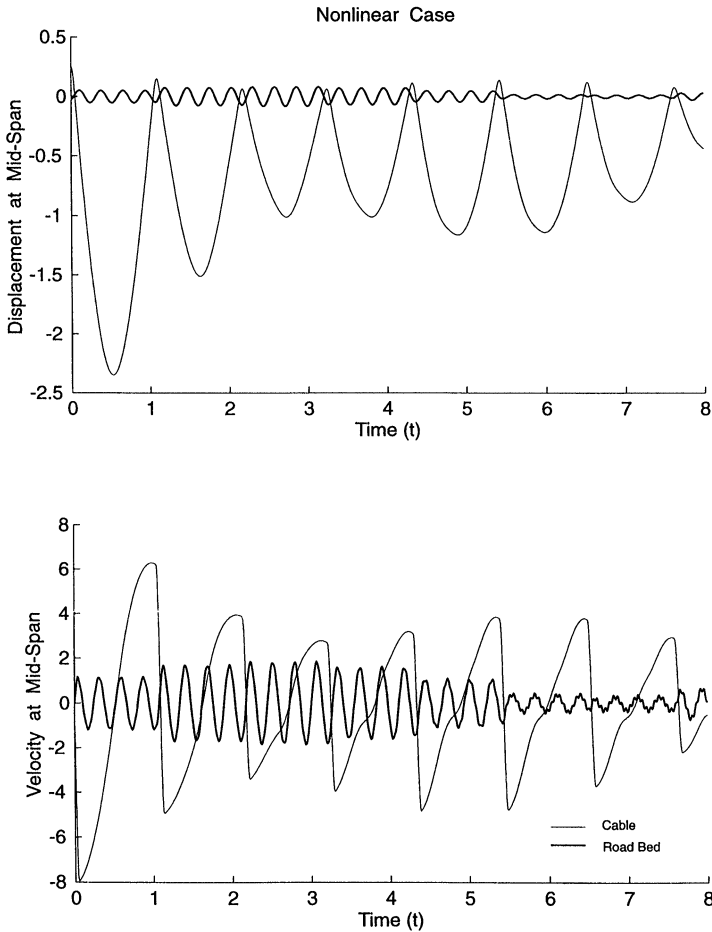


FIGURE 7 Displacement & velocity for  $\gamma_2 = 10^{-3}$ .

FIGURE 8 Displacement & velocity for  $\gamma_2 = 10^{-5}$ .

indefinitely improved by simply increasing the damping coefficient, thereby supporting the theory presented in Section 3.

#### (4C) Decay Rate vs Structural Damping $\gamma_{12}$

In the presence of structural damping alone ( $\gamma_1 = 0, \gamma_2 = 0$ ), similar conclusions as in (4A) and (4B) hold. The results are shown in Figs. 9 and 10 for linear and nonlinear systems respectively. The

	$\gamma_1$	$\gamma_2$	$\gamma_{12}$
a:	0	0	0
b:	0	0	$10^{-5}$
c:	0	0	$10^{-4}$
d:	0	0	$10^{-3}$
e:	0	0	$10^{-2}$

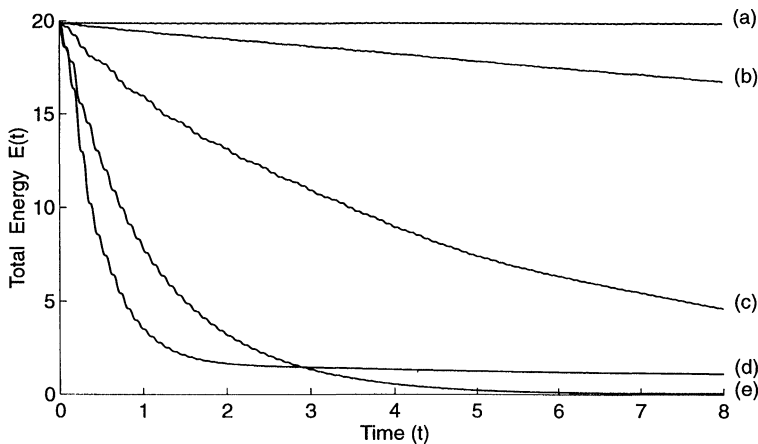


FIGURE 9 Linear case with structural damping ( $\gamma_{12}$ ).

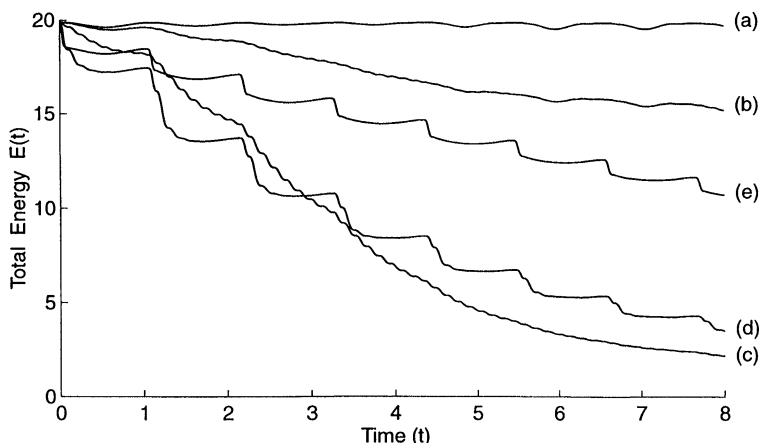


FIGURE 10 Nonlinear case with structural damping ( $\gamma_{12}$ ).

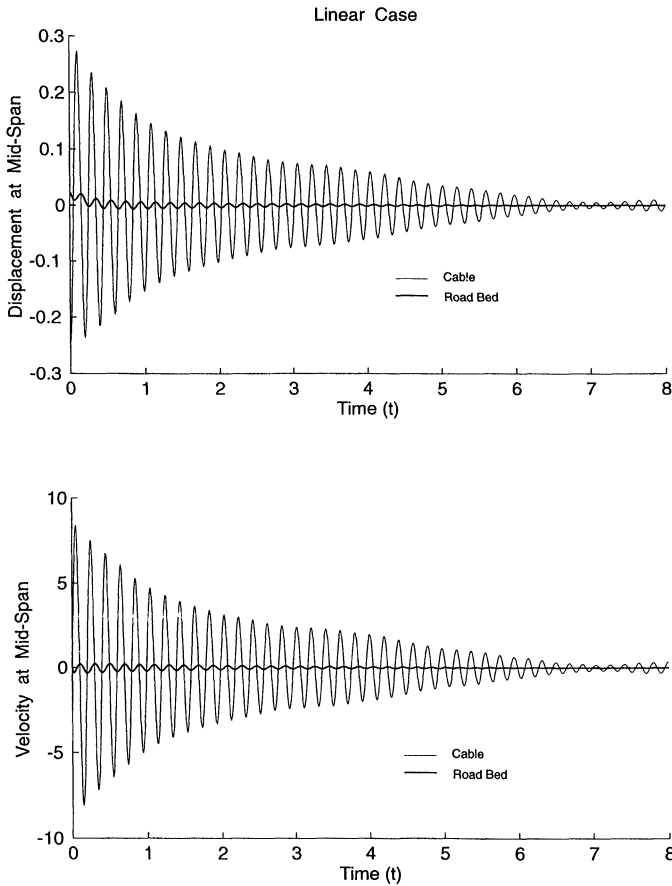


FIGURE 11 Displacement & velocity for  $\gamma_{12} = 10^{-2}$ .

corresponding displacements and their rates are also shown in Figs. 11 and 12. Again there is an optimum value for the structural damping  $\gamma_{12}$  as evidenced by the results shown for increasing values of  $\gamma_{12}$  starting from zero indicated by the graphs a  $\rightarrow$  b  $\rightarrow$  c  $\rightarrow$  d  $\rightarrow$  e. Again this supports the theory presented in Section 3.

#### **(4D) Structural Damping and Viscous Damping Combined**

Here we assume that both aerodynamic and structural damping are present. This is however the most realistic situation. Assuming the

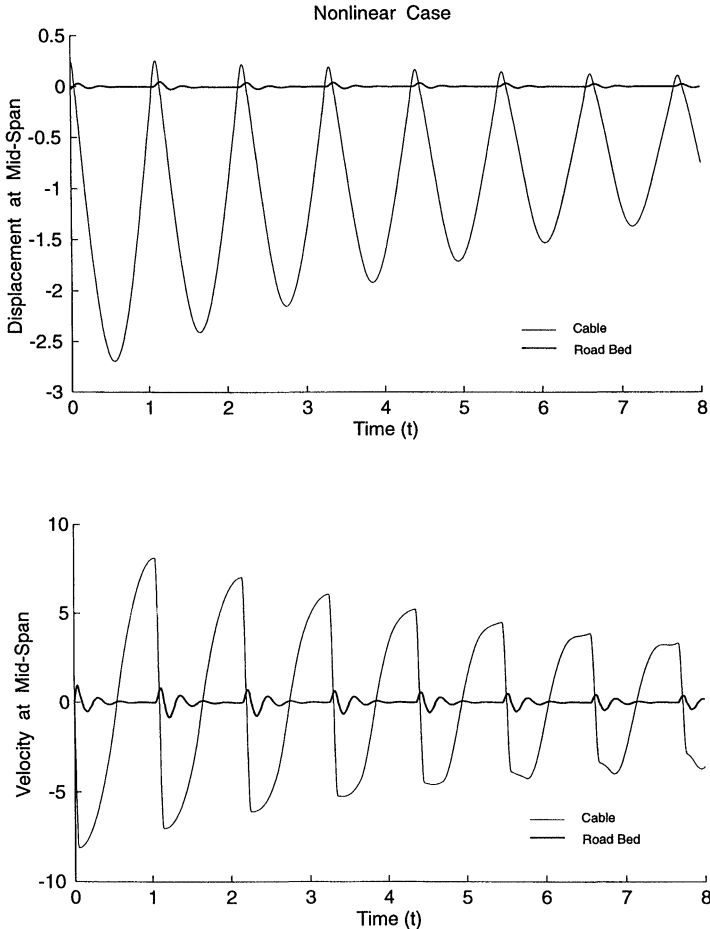
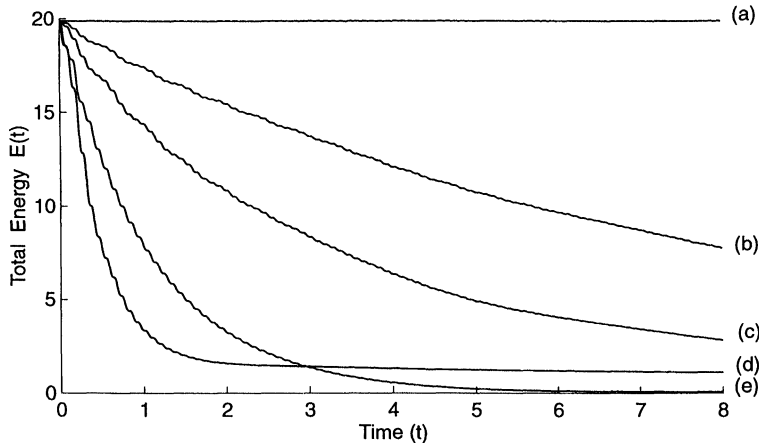
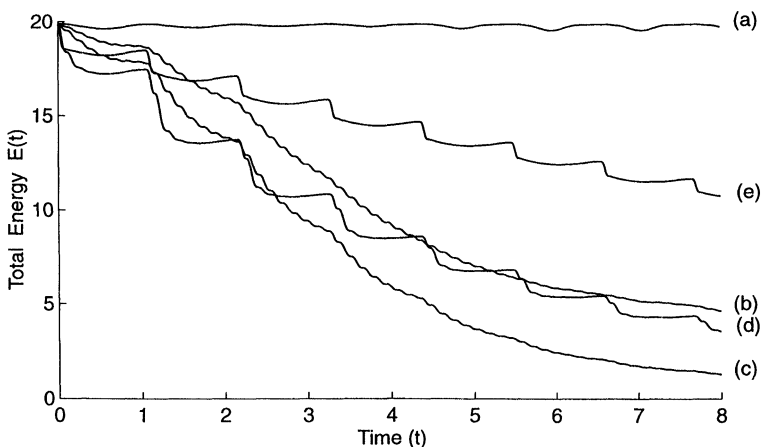
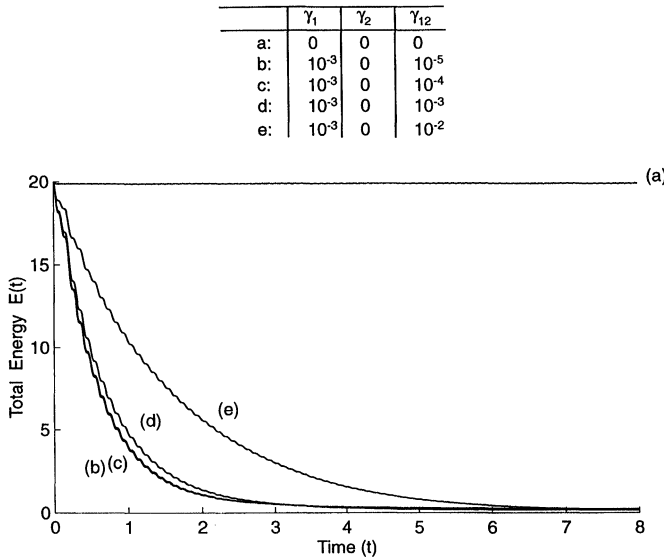
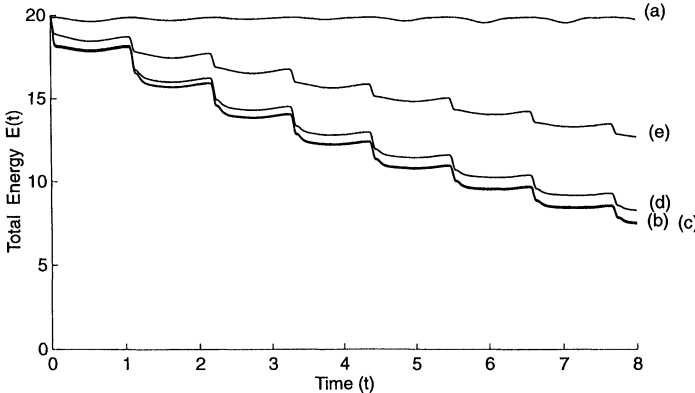


FIGURE 12 Displacement & velocity for  $\gamma_{12} = 10^{-4}$ .

aerodynamic damping provided by the suspension cables negligible ( $\gamma_2 = 0$ ) and fixing the aerodynamic damping for the road bed at  $\gamma_1 = 10^{-5}$ , we plot the Figs. 13 and 14 to show the energy decay with increasing structural damping for linear and nonlinear systems respectively. Again there is a critical value at which the decay rate is maximum. Increasing the value of  $\gamma_1$  to  $\gamma_1 = 10^{-3}$ , similar results are plotted in Figs. 15 and 16. In the linear case, comparing Figs. 13 and 15, we observe some improvement in the overall decay rate, but for the

	$\gamma_1$	$\gamma_2$	$\gamma_{12}$
a:	0	0	0
b:	$10^{-5}$	0	$10^{-5}$
c:	$10^{-5}$	0	$10^{-4}$
d:	$10^{-5}$	0	$10^{-3}$
e:	$10^{-5}$	0	$10^{-2}$

FIGURE 13 Linear case with damping ( $\gamma_1$  &  $\gamma_{12}$ ).FIGURE 14 Nonlinear case with damping ( $\gamma_1$  &  $\gamma_{12}$ ).

FIGURE 15 Linear case with damping ( $\gamma_1$  &  $\gamma_{12}$ ).FIGURE 16 Nonlinear case with damping ( $\gamma_1$  &  $\gamma_{12}$ ).

nonlinear systems, comparing Figs. 14 and 16 we observe decline. Since the decay rate  $d$  is a complicated function of the aerodynamic and structural damping coefficients,  $d \equiv d(\gamma_1, \gamma_2, \gamma_{12})$ , maximizing this with respect to one of the variables keeping the others fixed will not yield the optimum. This requires much more elaborate computational

efforts. However given the aerodynamic coefficients,  $\gamma_1$ ,  $\gamma_2$ , and the metallurgical constraints, it is relatively easy to determine the optimum structural damping coefficient as demonstrated in (4C).

## 5. CONCLUDING REMARKS

In this paper we have used a simplified (PDE) model for suspension bridge as proposed originally by Lazer and McKenna [1]. A complete mathematical analysis of this system was recently presented by the present authors [17,18]. Here we have used the results presented in [17] to study stability properties of the system. We have provided numerical results illustrating the comparative effectiveness of aerodynamic and structural damping. We have demonstrated both theoretically and by numerical simulation results that the decay rate cannot be indefinitely increased by simply increasing the aerodynamic or structural damping coefficients. There is an optimum value for these parameters.

## References

- [1] A.C. Lazer and P.J. McKenna, Large-amplitude periodic oscillations in suspension bridge: Some new connections with nonlinear analysis, *SIAM Rev.* **32**, 537–78, 1990.
- [2] O.H. Amann, T. Von Karman and G.B. Woodruff, The Failure of the Tacoma Narrows Bridge, Federal Works Agency, 1941.
- [3] F. Bleich, C.B. McCullough, R. Rosecrans and G.S. Vincent, The Mathematical Theory of Suspension Bridges. U.S. Dept. of Commerce, Bureau of Public Roads, 1950.
- [4] E.G. Wiles, Report of Aerodynamic Studies on Proposed San Pedro-Terminal Island Suspension Bridge, California, Bridge Research Branch, Division of Physical Research, Bureau of Public Roads, U.S. Dept. of Commerce, Washington, D.C., 1960.
- [5] A. Selberg, Oscillation and aerodynamic stability of suspension bridges, *Acta Polytechnica Scandinavica*, Series No. 13, 308–377, 1961.
- [6] A.M. Abdel-Ghaffer, Suspension bridge vibration: Continuum formation, *J. Engrg. Mech.* **108**, 1215–1232, 1982.
- [7] T. Kawada and A. Hirai, Additional mass method – A new approach to suspension bridge rehabilitation, *Official Proceedings, 2nd Annual International Bridge Conference*. Engineers of Society of Western Pennsylvania, 1985.
- [8] P.J. McKenna and W. Walter, Nonlinear oscillation in a suspension bridge, *Arch. Rational Mech. Anal.* **98**, 167–177, 1987.
- [9] A.C. Lazer and P.J. McKenna, Large scale oscillation behavior in loaded asymmetric systems, *Ann. Inst. H. Poincaré, Analyse Nonlinéaire* **4**, 244–274, 1987.
- [10] J. Glover, A.C. Lazer and P.J. McKenna, Existence and stability of large scale nonlinear oscillations in suspension bridges, *Journal of Applied Mathematics and Physics (ZAMP)* **40**, 172–200, 1989.

- [11] P.J. McKenna and W. Walter, Traveling waves in a suspension bridge, *SIAM J. Appl. Math.* **50**(3), 703–715, 1990.
- [12] Y.S. Choi, K.C. Jen and P.J. McKenna, The structure of the solution set for periodic oscillation in a suspension bridge model, *IMA Journal of Applied Mathematics* **47**, 283–306, 1991.
- [13] Daniela Jäger and P.J. McKenna, Nonlinear torsional flexings in a periodically forced suspended beam, *Journal of Computational and Applied Mathematics* **52**, 241–265, 1994.
- [14] N.U. Ahmed and S.S. Lim, Modeling and control of flexible space stations (slew maneuvers), *Proceedings of the 3rd Annual Conference on Aerospace Computational Control* (Eds. D.E. Bernard and G.K. Mann), JPL, NASA Pub. 89–45, Vol. 2, pp. 900–914.
- [15] N.U. Ahmed and S.K. Biswas, Mathematical modeling and control of large space structures with multiple appendages, *J. Math. Comput. Modeling* **10**(12), 891–900, 1988.
- [16] Peng Li and N.U. Ahmed, On exponential stability of infinite dimensional systems with bounded or unbounded perturbations, *Applicable Analysis* **30**, 175–187, 1988.
- [17] N.U. Ahmed and H. Harbi, Mathematical analysis of dynamic models of suspension bridge, *SIAM J. of Applied Mathematics* **58**(3), 1998.
- [18] N.U. Ahmed and H. Harbi, Dynamic Models of Suspension Bridge and their Stability, *Proc. of the IASTED International Conference, Control 97*, Cancun, Mexico (May 28–31, 1997), 386–390.
- [19] R. Temam, *Infinite-Dimensional Dynamical Systems in Mechanics and Physics*, Applied Mathematical Sciences Series, Vol. 68, Springer-Verlag, New York, Berlin, Heidelberg, London, Paris, Tokyo, 1988.

## Special Issue on Intelligent Computational Methods for Financial Engineering

### Call for Papers

As a multidisciplinary field, financial engineering is becoming increasingly important in today's economic and financial world, especially in areas such as portfolio management, asset valuation and prediction, fraud detection, and credit risk management. For example, in a credit risk context, the recently approved Basel II guidelines advise financial institutions to build comprehensible credit risk models in order to optimize their capital allocation policy. Computational methods are being intensively studied and applied to improve the quality of the financial decisions that need to be made. Until now, computational methods and models are central to the analysis of economic and financial decisions.

However, more and more researchers have found that the financial environment is not ruled by mathematical distributions or statistical models. In such situations, some attempts have also been made to develop financial engineering models using intelligent computing approaches. For example, an artificial neural network (ANN) is a nonparametric estimation technique which does not make any distributional assumptions regarding the underlying asset. Instead, ANN approach develops a model using sets of unknown parameters and lets the optimization routine seek the best fitting parameters to obtain the desired results. The main aim of this special issue is not to merely illustrate the superior performance of a new intelligent computational method, but also to demonstrate how it can be used effectively in a financial engineering environment to improve and facilitate financial decision making. In this sense, the submissions should especially address how the results of estimated computational models (e.g., ANN, support vector machines, evolutionary algorithm, and fuzzy models) can be used to develop intelligent, easy-to-use, and/or comprehensible computational systems (e.g., decision support systems, agent-based system, and web-based systems)

This special issue will include (but not be limited to) the following topics:

- **Computational methods:** artificial intelligence, neural networks, evolutionary algorithms, fuzzy inference, hybrid learning, ensemble learning, cooperative learning, multiagent learning

- **Application fields:** asset valuation and prediction, asset allocation and portfolio selection, bankruptcy prediction, fraud detection, credit risk management
- **Implementation aspects:** decision support systems, expert systems, information systems, intelligent agents, web service, monitoring, deployment, implementation

Authors should follow the Journal of Applied Mathematics and Decision Sciences manuscript format described at the journal site <http://www.hindawi.com/journals/jamds/>. Prospective authors should submit an electronic copy of their complete manuscript through the journal Manuscript Tracking System at <http://mts.hindawi.com/>, according to the following timetable:

Manuscript Due	December 1, 2008
First Round of Reviews	March 1, 2009
Publication Date	June 1, 2009

### Guest Editors

**Lean Yu**, Academy of Mathematics and Systems Science, Chinese Academy of Sciences, Beijing 100190, China; Department of Management Sciences, City University of Hong Kong, Tat Chee Avenue, Kowloon, Hong Kong; [yulean@amss.ac.cn](mailto:yulean@amss.ac.cn)

**Shouyang Wang**, Academy of Mathematics and Systems Science, Chinese Academy of Sciences, Beijing 100190, China; [sywang@amss.ac.cn](mailto:sywang@amss.ac.cn)

**K. K. Lai**, Department of Management Sciences, City University of Hong Kong, Tat Chee Avenue, Kowloon, Hong Kong; [mskklai@cityu.edu.hk](mailto:mskklai@cityu.edu.hk)